EPJ Web of Conferences **322**, 09001 (2025) https://doi.org/10.1051/epjconf/202532209001
*CNR*24*

Nuclear inputs relevant to nuclear astrophysics, status and perspectives

Stéphane Goriely[1,2,*], *Wouter* Ryssens[1,2,**], *Stéphane* Hilaire[3,4,***], and *Sophie* Péru[3,4,****]

[1]Institute of Astronomy and Astrophysics, Université Libre de Bruxelles, CP 226, B-1050 Brussels, Belgium
[2]Brussels Laboratory of the Universe - BLU-ULB, Université Libre de Bruxelles, 50 Av. Franklin Roosevelt, B-1050 Brussels, Belgium
[3]CEA, DAM, DIF, F-91297 Arpajon, France
[4]Université Paris-Saclay, CEA, LMCE, 91680 Bruyères-le-Châtel, France

Abstract. Nuclear physics influences are present throughout the Universe at every scale. Over the past decades, significant efforts have been dedicated to various fields related to nucleosynthesis and stellar evolution. These include both experimental and theoretical nuclear physics, as well as ground- and space-based astronomical observations and astrophysical modeling. Despite numerous successes, major challenges and unresolved questions persist. Concerning nuclear physics, despite the remarkable efforts of experimentalists in studying unstable targets, it remains unlikely that we will be able to measure the structure and interaction properties of all astrophysically relevant nuclei in the near future. Therefore, further progress must rely on theoretical approaches. The necessary ingredients (properties of cold and hot nuclei, nuclear level densities, optical potentials, photon strength functions, fission properties, β-strength functions) should ideally be derived from *global*, *universal* and *microscopic* models. New progress based on mean-field models are described and their impact on nuclear reaction rates of astrophysical relevance discussed and on nucleosynthesis illustrated.

1 Introduction

The Universe is pervaded with nuclear physics imprints at all scales [1, 2]. Important efforts have been devoted during the last decades to the different fields related to nucleosynthesis and stellar evolution, especially in experimental and theoretical nuclear physics, as well as in ground- or space-based astronomical observations and astrophysical modellings. In spite of many successes, major problems and puzzles remain.

Figure 1 illustrates the various nuclear data needs for stellar structure, stellar evolution and nucleosynthesis applications [1]. These include the big-bang nucleosynthesis [4], the production of Li-Be-B by galactic cosmic rays (in particular C, N, O elements interacting with protons and α-particles) [5], hydrostatic and explosive burning stages of stellar evolution, the composition of the crust of neutron stars (NSs) [6], the rapid proton-capture process (or rp-process) in X-ray bursts [7], the suggested νp process in exploding massive stars [8] as well as different nucleosynthesis processes responsible for the production of elements heavier than iron, such as the slow neutron-capture process (or s-process) [9], the intermediate neutron-capture process (or i-process) [10], the rapid-neutron capture process (or r-process) [11] and the p-process [12].

Experimental nuclear data only cover a minute fraction of the whole set of data required for such applications. Reactions of interest often concern unstable or even exotic (neutron-rich, neutron-deficient, superheavy) species for which no experimental data exist. In addition, a large number (thousands) of unstable nuclei may be involved for which many different properties have to be determined (Fig. 1). The energy range for which measurements are available is also restricted to the small range reachable by contemporary experimental setups. An additional serious difficulty comes from the fact that the nuclei are immersed in stellar environments which may have a significant impact on their static properties and the diversity and relative probabilities of their transmutation modes. The description of nuclei as individual entities has even to be replaced by the construction of an equation of state (EoS) at high enough temperatures and/or densities prevailing in the cores of exploding stars and in NSs. Despite the remarkable efforts of experimentalists in considering unstable targets and pushing ever closer to the neutron drip line [13–15], there is unfortunately little hope of measuring the structure and interaction properties of all the astrophysically relevant nuclei in the foreseeable future. For further progress one has to turn to theory. Only a few theoretical aspects are discussed in this contribution. Readers are referred to reviews, such as Ref. [1, 16], for more information on the many open questions affecting nuclear astrophysics.

All the mentioned nuclear astrophysics applications require a large amount of nuclear data, but not all of the latter play a crucial role. To estimate the impact of nuclear inputs on astrophysical observables, simulations are usually performed making use of different nuclear ingredients entering the calculation of reaction rates (see e.g. Fig. 2).

*e-mail: stephane.goriely@ulb.be
**e-mail: wouter.ryssens@ulb.be
***e-mail: stephane.hilaire@cea.fr
****e-mail: sophie.peru-desenfants@cea.fr

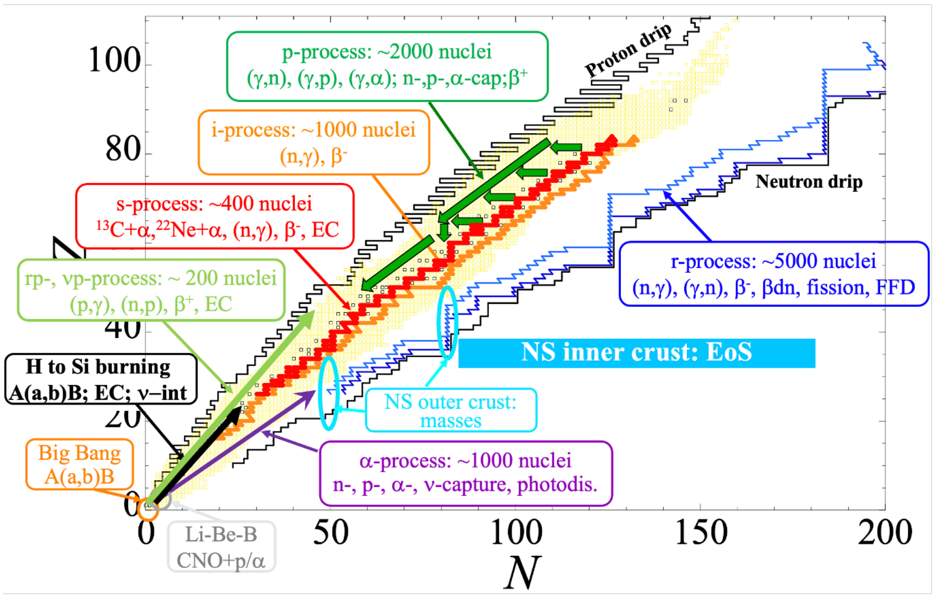

Figure 1. Schematic representation in the (N, Z) plane of the different astronuclear physics applications, including nucleosynthesis processes, composition and structure properties of NSs. For each process, the nuclear data needs are sketched. The open black squares correspond to stable or long-lived nuclei, the yellow squares to the nuclei for which masses have been measured and are included in the 2020 Atomic Mass Evaluation (AME) [3]. Nuclei with a neutron or proton separation energies tending to zero define the neutron or proton "drip lines" (solid black lines), as predicted from a mass model. More details can be found in Ref. [1].

However, as detailed in some works, drawing conclusions on the relevance of given nuclear reaction or decay rates on astrophysical observables is far from being an easy task [see e.g. the application to the i-process nucleosynthesis in Ref. 17]. In particular, nuclear predictions are affected by correlated model (also referred to as systematic) as well as uncorrelated parameter (sometimes called "statistical") uncertainties. The former ones are known to dominate for unstable experimentally unknown nuclei [e.g., 18] since there is usually no or very little experimental information available to constrain the model on those nuclei. Whenever experimental observables (with uncertainties) are available, either for rates or reaction model ingredients, they constrain the theoretical predictions. In this case, they also limit the possible range of variation of the model parameters and reduce the impact on model as well as parameter uncertainties. However, for exotic nuclei, models of different natures, ranging between macroscopic to microscopic approaches [e.g., 11, 19–21], may provide rather different predictions, but such model uncertainties remain correlated (by the model) and can consequently not be propagated into astrophysical models with Monte Carlo techniques. Closer to the experimentally known region, uncorrelated parameter uncertainties may be significant, e.g. in the description of the i-process nucleosynthesis [17]. In all cases, when propagating the nuclear uncertainties into nucleosynthesis models, it is of paramount importance to ensure that astrophysical models as realistic as possible are considered and properly described by a representative number of trajectories or shells. One-zone models or simplified propagation with a restricted number of trajectories often give an erroneous picture of the astrophysical site and propagating nuclear uncertainties in such conditions leads to incorrect conclusions regarding the impact and the relevance of nuclear reaction or decay rates [17, 22].

2 Theoretical predictions for nucleosynthesis applications

Predictions of astrophysical reaction rates remain strongly affected by uncertainties, as shown in Fig. 2. For astrophysical applications, the necessary ingredients (properties of cold and hot nuclei, nuclear level densities (NLD), optical potentials, photon strength functions (PSF), fission properties, β-strength functions) should ideally be derived from *global*, *universal* and *microscopic* models [1]. The large number of nuclides involved in the modelling of some nucleosynthesis mechanisms demands the use of global models. On the other hand, a universal description of all nuclear properties within a unique framework for all nuclei involved ensures the essential coherence of the predictions of all unknown data. Finally, a microscopic description provided by a physically sound theory based on first principles ensures extrapolations away from experimentally known energy or mass regions that are likely to be more reliable than predictions derived from more or less parametrized approaches of various types and levels of sophistication. Nowadays, microscopic models can be tuned to the same level of accuracy as the phenomenological models, and therefore could replace the phenomenological inputs in practical applications. Some progress made in the last years concerning some of the key ingredients needed to estimate reaction cross sections and astrophys-

 https://doi.org/10.1051/epjconf/202532209001

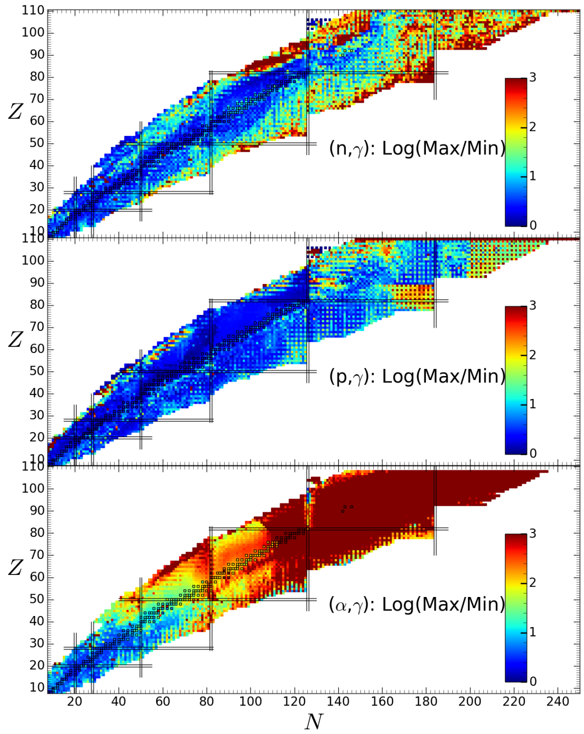

Figure 2. Representation in the (N, Z) plane of the model uncertainties affecting the radiative n-, p- and α-capture rates at a temperature $T = 2\ 10^9$ K. The colour code represents the ratios between the maximum and minimum astrophysical rates obtained with the TALYS code [23] using different models for masses, level densities, photon strength functions and optical potentials.

ical rates are reviewed below. These concern the nuclear structure properties, NLD, PSF, fission and optical potential.

2.1 Nuclear structure properties

Many effective interactions within the relativistic or non-relativistic mean-field approaches have been proposed to estimate nuclear structure properties [24]. Only the BSk [25] and BSkG [26, 27] effective interactions at the origin of Skyrme-HFB mass models and the D1M interaction at the origin of the Gogny-HFB mass model [28] have been fitted to the complete set of experimental masses with a root-mean-square (rms) deviations lower than typically 0.8 MeV and can consequently be considered for astrophysics applications. This contrasts with the many other Skyrme or Gogny interactions giving rise to mass predictions with an rms deviation typically far larger than 2–3 MeV with respect to the bulk of known masses. With such a low accuracy, these mass models should not be used for nuclear astrophysics applications. Additionally, other global mass models have been developed, essentially within the macroscopic-microscopic approach, but this approach remains unstable with respect to parameter variations, as shown in the framework of the droplet model [29] and as illustrated in Fig. 3 between the FRDM12 [30] and WS4 [31] mass models, especially when approaching the neutron drip line where deviations up to 15 MeV can be found. In addition, this approach suffers from major shortcomings, such as the incoherent link between the macroscopic part and the microscopic correction or the instability of the shell correction [32, 33]. For this reason, more fundamental approaches, such as those based on energy density functionals are needed (provided they accurately describe relevant observables).

Recently, a new family of Skyrme-HFB models (BSkG) has been constructed using a three-dimensional coordinate-space representation, allowing for axial, triaxial and octupole deformations during the adjustment process [26, 27, 35]. In addition, while nuclei with an odd number of nucleons were traditionally described within the so-called equal filling approximation, the BSkG3 mass model [27] treat them on the same footing as even-even nuclei by breaking time-reversal symmetry. BSkG3 also offers a stiff equation of state of pure neutron matter (supporting a maximum NS mass of 2.26 $M_\odot$) and makes use of a "realistic" microscopic pairing. The final rms deviation of BSkG3 amounts to 0.63 MeV with respect to the 2457 known masses [3] making it suitable for astrophysics application. It also reproduces the 45 empirical primary barriers [36] (*i.e.* the highest barriers of prime interest in cross section calculations) of $Z \geq 90$ nuclei with an rms deviation as low as 0.33 MeV, as discussed in Sec. 2.4.

Similarly, HFB mass models have been recently extended making use of a finite-range Gogny interaction characterized by three ranges [34]. The new D3G3M interaction reproduces the 2457 masses with an rms deviation of 0.87 MeV and describe the equation of state of pure neutron matter with a stiffness significantly larger than D1M [28] supporting a maximum NS mass of 2.14 $M_\odot$.

When considering mass models obtained in relatively different frameworks, e.g the Skyrme-HFB or Gogny-HFB mass models, deviations are also found in the mass predictions away from the experimentally known region. For example, as shown in Fig. 3, deviations up to typically ±5 MeV can be observed for exotic nuclei between HFB-31 [25], D1M [28], D3G3M [34], and BSkG3 [27], especially around the $N = 126$ and 184 shell closures. Such differences mainly stem from different properties of the interaction, including the symmetry energy, the effective mass, the pairing description, the spin-orbit force, ..., as studied in detail through the series of HFB mass models [25]. Neutron capture rates can consequently deviate by 3 to 5 orders of magnitude with such mass differences, essentially due to different local variations in the pairing and shell description. Such deviations by far exceeds what is acceptable for nucleosynthesis applications. For this reason, further improvements of mass models are required. These include development of relativistic as well as non-relativistic mean field models, but also the inclusion within such approaches of the state-of-the-art beyond-mean-field corrections, like the quadrupole or octupole correlations by the Generator Coordinate Method [37, 38] and a proper treatment of odd-A and odd-odd nuclei with time-reversal symmetry breaking [26]. In addition to an accurate prediction of the known masses, such models should also aim for an accurate description of as many other (pseudo-) observ-

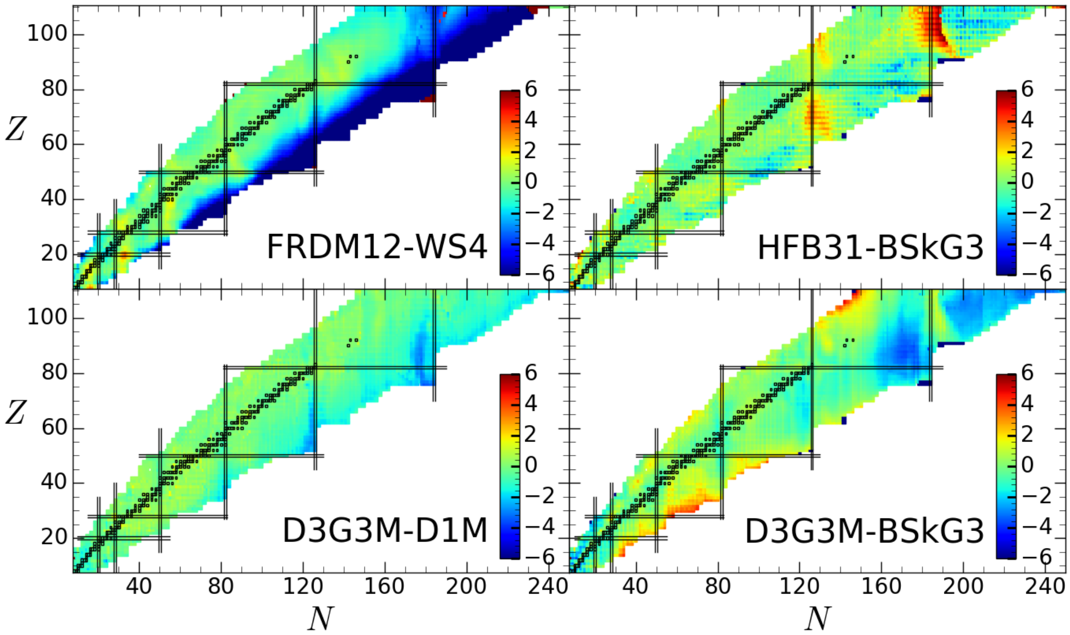

Figure 3. Representation in the (N, Z) plane of the mass differences (in MeV) between FRDM12 [30], WS4 [31], as well as HFB-31 [25], D1M [28], D3G3M [34] and BSkG3 [27] models for all the 8500 nuclei from $Z = 8$ up to $Z = 110$ between the BSkG3 proton and neutron driplines. The open squares correspond to the valley of β-stability. The double solid lines depict the neutron and proton magic numbers. Note that the mass differences are limited to ±6 MeV, larger values are included in the upper and lower bounds.

ables as possible. These include charge radii and neutron skin thicknesses, fission barriers and shape isomers, spectroscopic data such as the 2^+ energies, moments of inertia, but also infinite (neutron and symmetric) nuclear matter properties obtained from realistic calculations as well as specific observed or empirical properties of NSs, like their maximum mass or mass-radius relations [6, 39].

The impact of various mass models on the heavy nuclei composition of the material ejected by a NS merger is illustrated in Fig. 4 for the specific end-to-end simulation of the 1.375 – 1.375 $M_\odot$ NS-NS binary system [40]. The same six different mass models as in Fig. 3 are considered. They all reproduce known masses with an rms deviation better than 0.8 MeV. Four are based on the HFB mean-field approach and two (FRDM12 and WS4) on the macroscopic-microscopic one. Globally, the 6 mass models are seen to give rise to abundance distributions that agree with each other and match relatively well the solar system r-distribution for nuclei with $90 \lesssim A \lesssim 130$. However, some local differences by a factor of 4, in either direction, can be found among them, in particular in the vicinity of $A \simeq 180$, $A \simeq 200$ and for the Th and U production.

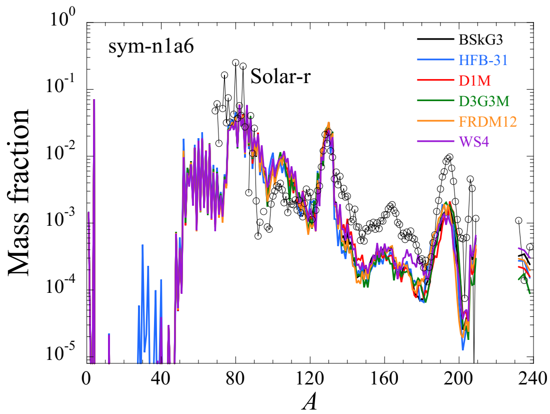

Figure 4. Final mass fractions of the material ejected as a function of the atomic mass A for the end-to-end 1.375 – 1.375 $M_\odot$ NS-NS simulation (the so-called sym-n1a6 model) [40]. The results are obtained with 6 different mass models in the calculation of the radiative neutron capture and photoneutron rates, namely BSkG3 [27], HFB-31 [25], D1M [28], D3G3M [34], FRDM12 [30], and WS4 [31]. The solar system r-abundance distribution (open circles) from [41] is shown for comparison and arbitrarily normalised.

2.2 Nuclear level densities

NLDs play a key role in many nuclear applications. When considering publicly available global NLD models providing predictions for the large number of nuclei involved in nucleosynthesis applications, only a limited number of methods and results are available [23, 36]. Recent progress using the combinatorial approach [42] built on the BSkG3 ground states has been proposed [43]. The added value comes not only from the new BSkG3 Skyrme and pairing

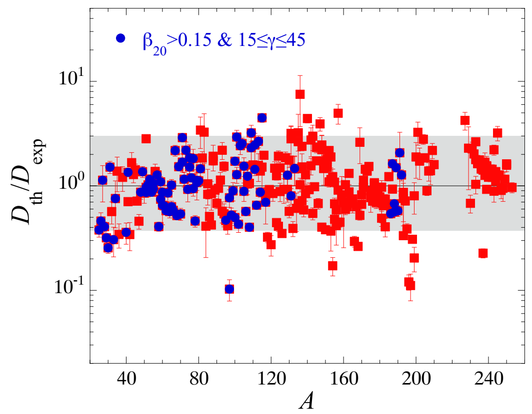

Figure 5. comparison of s-wave resonance spacings calculated with BSkG3 plus combinatorial approach and experimental values [36]. The blue dots correspond to triaxially deformed nuclei with $\beta_{20} > 0.15$ and $15° < \gamma < 45°$.

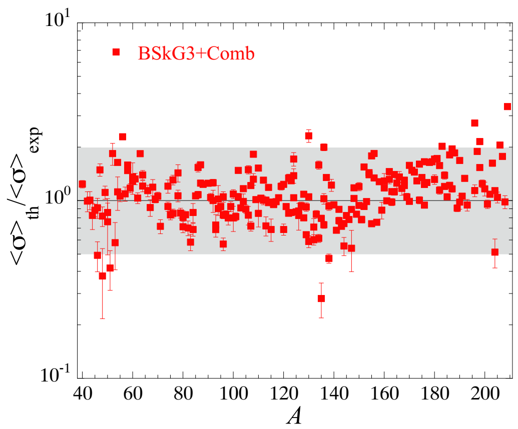

Figure 6. Comparison of Maxwellian-averaged (n,γ) cross sections at $kT = 30$ keV calculated with BSkG3 plus combinatorial NLD with experimental data [45] for nuclei with $40 \leq A \leq 209$.

description but also from taking into account the possible triaxiality of the ground state, which can either increase or decrease the nuclear level density with respect to the axially deformed case depending on the magnitude of the deformation. In particular, for strongly deformed nuclei and large moment of inertia, triaxiality tends to increase the total density due to the additional collective enhancement. This is not the case for modest deformations where the smaller single-particle level density at triaxial deformations gives rise to a decrease of the total density. The overall description of the experimental s-wave spacings at the neutron separation energy are shown in Fig. 5. When applied to the calculation of the Maxwellian-averaged cross section (MACS), these NLD also give rise to a good agreement with experimental data, as illustrated in Fig. 6.

To go beyond the usual particle-independent approximation, a conceptually new approach based on the boson expansion of QRPA excitations has been recently proposed [16, 44]. The calculated nuclear level densities follow an energy dependence close to a constant-temperature formula at energies above a few MeV, but present a rather narrow spin distribution. More details can be found in Hilaire et al. (These proceedings).

2.3 Photon strength function

Major recent progress has also been made in the determination of de-excitation photon strength function both within the shell model [46, 47] and QRPA (Péru et al., these proceedings) approaches. As shown in Fig. 7, within the D1M+QRPA approach, it is possible to estimate the E1 and M1 PSF between excited states, and more particularly from a given excitation energy U as a function of the photon energy E_γ. Such a PSF includes also the contribution to the ground state that can be seen to be equal to the photoabsorption PSF from the ground state to the excite state at energy U, as deduced from the reciprocity theorem. While the E1 de-excitation PSF is in rather good agreement with the photoabsorption PSF, still some deviation can be observed but without any particularly strong enhancement at the lowest energies E_γ. In contrast for the M1 PSF, a significant increase at decreasing E_γ (the so-called "upbend") is found and a lower strength is quite systematically obtained for $E_\gamma \gtrsim 3$ MeV. As an application, the MACS has been estimated with the TALYS code [23] taking into account the strong U dependence of the PSF. For this particular case, the de-excitation E1 and M1 PSF for $U \simeq 6-7$ MeV $\lesssim S_n = 7.46$ MeV is found to be lower than the photoabsorption PSF, leading to a decrease of the MACS. Some more details can be found in Péru et al. (these proceedings).

2.4 Fission

The HFB model has proven its capacity to estimate the fission barrier height with a relatively high degree of accuracy [26, 36, 49–51]. Recent progress has been made and state-of-the-art HFB predictions also include fission barriers in the observables to which the effective interaction is optimised. As for masses, the BSkG3 energy density functional has been applied to the calculation of fission properties. Relying on a flexible three-dimensional coordinate representation of the nucleus, the model takes into account both triaxial and octupole deformations and time-reversal symmetry breaking. In addition to the excellent description of known masses (see Sect. 2.1), the BSkG3 model also reproduces all empirical values for the fission barriers as well as isomer excitation energies of actinide nuclei with unprecedented accuracy. In particular, the BSkG3 model [27] reproduces the 45 primary empirical barriers of nuclei with $90 \leq Z \leq 96$ with an rms deviation as low as 0.33 MeV. For the secondary barriers, an rms deviation of 0.51 MeV is obtained and for the shape isomer of 0.36 MeV. Such predictions represent a clear improvement

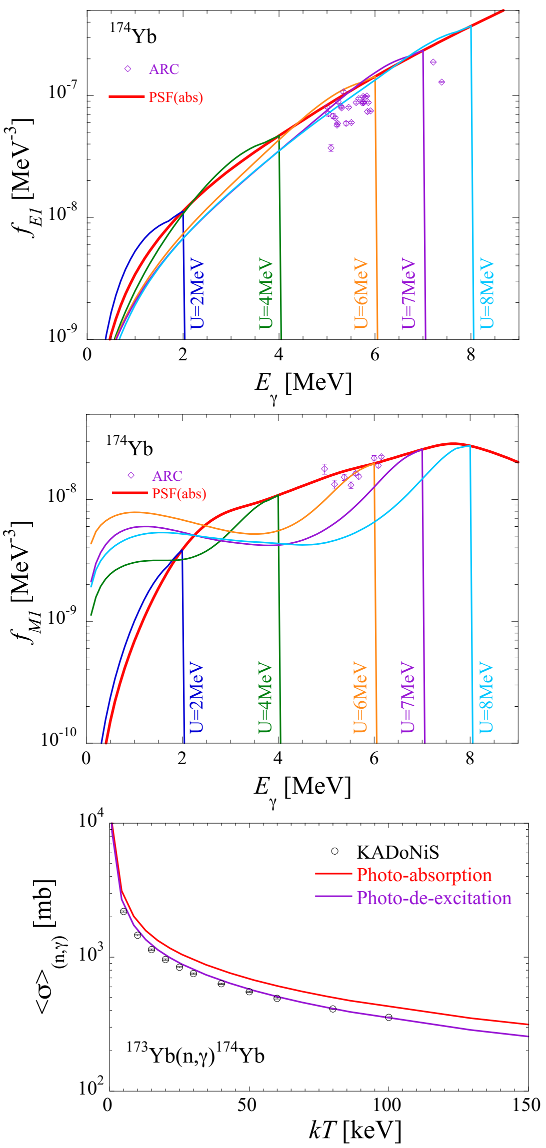

Figure 7. *Upper panel*: ^{174}Yb E1 PSF as a function of the photon energy E_γ. The thick red curve corresponds to the photoabsorption D1M+QRPA PSF and the colour lines to the de-excitation PSF (calculated within the same D1M+QRPA approach) from a given excitation energy U. ARC data from [48] are also shown. *Middle panel*: same as upper panel for the M1 PSF. *Lower panel*: ^{173}Yb$(n,\gamma)^{174}$Yb MACS calculated with the photoabsorption or de-excitation PSF as a function of the thermal energy kT and compared with experimental data [45].

with respect to most of the other large-scale macroscopic-microscopic or mean-field models. The success of BSkG3 is ascribed to (i) the inclusion of fission properties in the parameter adjustment and (ii) its highly general numerical representation of the nucleus that includes the possibility for combined triaxial and octupole deformations. BSkG3 fission paths of essentially all nuclei exploit triaxial deformation to lower both barriers significantly, combining a finite value of the triaxiality angle γ with finite octupole deformation near the outer barrier.

3 Optical potential

Though the phenomenological nucleon-nucleus optical potential of Woods-Saxon type [52] is still commonly used for astrophysical applications, it is often replaced by the more microscopic potential derived from a Reid's hard core nucleon-nucleon interaction by applying the Brückner-Hartree-Fock approximation [53]. This so-called JLM potential has been updated by Bauge et al. [54] (hence JLMB) who empirically renormalized the energy dependence of the potential depth to reproduce scattering and reaction observables for spherical and quasi-spherical nuclei between ^{40}Ca and ^{209}Bi in a large energy range from the keV region up to 200 MeV. However, the isovector contribution to the imaginary component remains unconstrained at the energies in the keV region. This can have a drastic impact on the radiative neutron capture rates of exotic neutron-rich nuclei and such an uncertainty will need to be addressed both experimentally and theoretically in the future. Readers are referred to Goriely (these proceedings) for a discussion on the isovector contribution to the imaginary JLMB component and its impact on both the astrophysical neutron capture rates and the r-process nucleosynthesis.

The situation for the α-particle-nucleus optical potential is much less satisfactory, and one still has to rely on phenomenological potentials. Most of the proposed potentials are derived from fits to elastic α-nucleus scattering data at relatively high energies, i.e. far above the Coulomb barrier (see e.g. [55]). However, the optical potential, and in particular its imaginary component, is known to be strongly energy dependent at energies below the Coulomb barrier. As a consequence, its extrapolation to sub-Coulomb energies is even more uncertain than in the case of nucleons, as illustrated by the ^{144}Sm$(\alpha,\gamma)^{148}$Gd case (Fig. 8). The development of a global α-nucleus optical potential to describe scattering and reaction cross sections at energies $E \lesssim 20$ MeV of better relevance to astrophysics has been attempted adopting a Woods-Saxon [55, 56] or a double folding [57–59] component of the real part. In all cases, a phenomenological form of the imaginary optical potential and of its energy dependence is still adopted. The resulting S-factors for 5 different optical potentials are shown in Fig. 8 showing the diversity of the predictions at Gamow energies of relevance to the p-process nucleosynthesis [12]. The uncertainties stemming from the α-particle-nucleus optical potential strongly propagates into our determination of the (α,γ) reaction rates, as also seen in Fig. 2 (lower panel).

As an illustration, we show in Fig. 9 the resulting overproduction factors of p-nuclei obtained in the supernova explosion of a rotating 25 $M_\odot$ star of $Z = 0.001$ metallicity (model M25Zm3V4B in Ref. [60]) obtained with 5 different optical potentials [55–59]. The production of $A \gtrsim 140$ p-nuclei remains highly affected by the adopted (γ,α) reaction rates, hence by the systematic uncertainties associated with the α-particle-nucleus optical potential, devi-

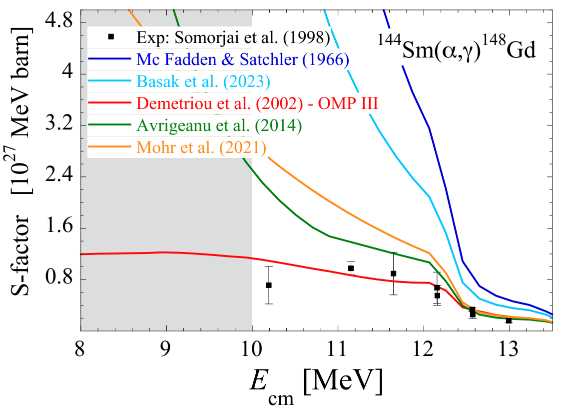

Figure 8. Comparison of ^{144}Sm(α,γ)^{148}Gd astrophysical S-factor measured at low energies [61] and calculated with different optical potentials [55–59]. The shaded area represents the Gamow energy range in p-process conditions.

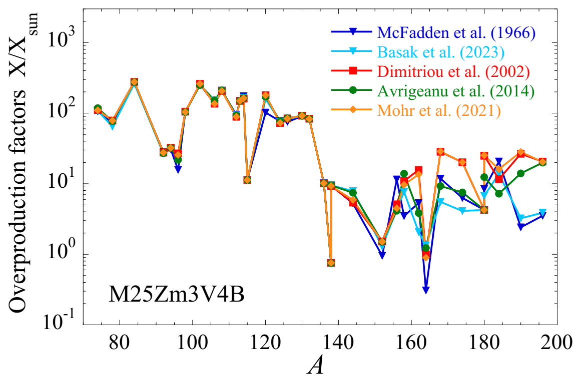

Figure 9. Overproduction factors of p-nuclei estimated in the explosion of a rotating 25 M$_\odot$ star of Z = 0.001 metallicity (model M25Zm3V4B in [60]) obtained with 5 different optical potentials [55–59].

ation up to a factor 10 being found in the ejecta yields. More details on the astrophysical model can be found in Ref. [60].

4 Conclusions

A huge amount of nuclear data for thousands of nuclei is needed for nuclear astrophysics applications. This challenges experimental techniques, but also the robustness and predictive power of the necessary nuclear models. For the last decades, important progress has been achieved both through new measurements and through the development of improved nuclear models. Despite such impressive progress, nuclear astrophysics still requires *(i)* dedicated experimental work on key reactions (such as ^{12}C+α, ^{12}C+^{12}C, ^{22}Ne+α, ^{17}O+α, ...), key properties (masses, charged radii, level densities, photon strength functions, optical potentials, fission probabilities, ...) for stable as well as unstable and exotic nuclei, and *(ii)* dedicated theoretical work based on models that are as "microscopic" as possible for experimentally inaccessible nuclei. Mean-field-based models are state-of-the-art in this respect, but they might be joined in the near future by ab-initio and shell model approaches. This effort to improve microscopic nuclear predictions is concomitant with new development aiming at improving the description of the reaction mechanisms, including the equilibrium, pre-equilibrium and direct capture processes. This theoretical work requires in parallel new measurements of structure properties far away from stability, but also reaction cross sections on stable targets and any experiments that can provide new insight on the numerous ingredients of the reaction models and their extrapolation far away from the valley of β-stability.

Acknowledgement

This work has been supported by the Fonds de la Recherche Scientifique (F.R.S.-FNRS; Belgium) under Grant No IISN 4.4502.19 as well as under the EOS Project No O022818F co-funded by the Research Foundation Flanders (FWO, Belgium). The computational resources have been provided by the Consortium des Equipements de Calcul Intensif (CECI), funded by the F.R.S.-FNRS under Grant No 2.5020.11 and by the Walloon Region.

References

[1] M. Arnould, S. Goriely, Prog. Part. Nucl. Phys. **112**, 103766 (2020). 10.1016/j.ppnp.2020.103766
[2] C. Iliadis, *Nuclear Physics of Stars*, second edition edn. (Wiley-VCH, 2015)
[3] M. Wang, et al., Chinese Physics C **45**, 030003 (2021). 10.1088/1674-1137/abddaf
[4] C. Pitrou, et al., Phys. Rep. **754**, 1 (2018). 10.1016/j.physrep.2018.04.005
[5] Y. Génolini,et al., Phys. Rev. C **98**, 034611 (2018). 10.1103/PhysRevC.98.034611
[6] A.F. Fantina,et al., Astron. Astrophys. **559**, A128 (2013). 10.1051/0004-6361/201321884
[7] J. José,et al.Astrophys. J. Suppl. S. **189**, 204 (2010). 10.1088/0067-0049/189/1/204
[8] C. Fröhlich,et al., Phys. Rev. Lett. **96**, 142502 (2006). 10.1103/PhysRevLett.96.142502
[9] F. Käppeler,et al., Rev. Mod. Phys. **83**, 157 (2011). 10.1103/RevModPhys.83.157
[10] A. Choplin, et al., Astron. Astrophys. **667**, A155 (2022). 10.1051/0004-6361/202244360
[11] M. Arnould,et al., Phys. Repts. **450**, 97 (2007). 10.1016/j.physrep.2007.06.002
[12] M. Arnould, S. Goriely, Phys. Repts. **384**, 1 (2003). 10.1016/S0370-1573(03)00242-4
[13] A. Stamatopoulos, et al., Nucl. Instrum. Methods Phys. Res. A **1025**, 166166 (2022). 10.1016/j.nima.2021.166166
[14] I. Dillmann,et al., Eur. Phys. J. A **59**, 105 (2023). 10.1140/epja/s10050-023-01012-9

[15] A. Spyrou, et al., Phys. Rev. Lett. **132**, 202701 (2024). 10.1103/PhysRevLett.132.202701
[16] S. Goriely, Eur. Phys. J. A **59**, 16 (2023). doi.org/10.1140/epja/s10050-023-00931-x
[17] S. Martinet, et al., Astron. Astrophys. **684**, A8 (2024). 10.1051/0004-6361/202347734
[18] S. Goriely, R. Capote, Phys. Rev. C **89**, 054318 (2014). 10.1103/PhysRevC.89.054318
[19] S. Goriely, Eur. Phys. J. A **51**, 172 (2015). 10.1140/epja/i2015-15172-2
[20] S. Hilaire, et al., Eur. Phys. J. A **52**, 336 (2016). 10.1140/epja/i2016-16336-2
[21] A. Plompen et al., eds., *Towards more accurate and reliable predictions for nuclear applications*, Vol. 146 of *EPJ Web of Conferences* (EDP Sciences, France, 2017)
[22] I. Kullmann,et al., MNRAS **523**, 2551 (2023). 10.1093/mnras/stad1458
[23] A. Koning, et al., Eur. Phys. J. A **59**, 131 (2023). 10.1140/epja/s10050-023-01034-3
[24] M. Bender,et al., Rev. Mod. Phys. **75**, 121 (2003). 10.1103/RevModPhys.75.121
[25] S. Goriely, et al., Phys. Rev. C **93**, 034337 (2016). 10.1103/PhysRevC.93.034337
[26] W. Ryssens,et al., Eur. Phys. J. A **58**, 246 (2022). 10.1140/epja/s10050-022-00894-5
[27] G. Grams, et al., Eur. Phys. J. A **59**, 270 (2023). 10.1140/epja/s10050-023-01158-6
[28] S. Goriely, et al., Phys. Rev. Lett. **102**, 242501 (2009). 10.1103/PhysRevLett.102.242501
[29] S. Goriely, M. Arnould, Astron. Astrophys. **262**, 73 (1992)
[30] P. Möller, et al., At. Data Nucl. Data Tables **109-110**, 1 (2016). 10.1016/j.adt.2015.10.002
[31] N. Wang,et al., Phys. Lett. B **734**, 215 (2014). 10.1016/j.physletb.2014.05.049
[32] J.M. Pearson, Hyp. Int. **132**, 59 (2001). 10.1023/A:1011973100463
[33] D. Lunney, et al., Rev. Mod. Phys. **75**, 1021 (2003). 10.1103/RevModPhys.75.1021
[34] L. Batail, et al., Phys. Rev. Lett. submitted (2024)
[35] G. Scamps,et al.Eur. Phys. J. A **57**, 333 (2021). 10.1140/epja/s10050-021-00642-1
[36] R. Capote,et al., Nuclear Data Sheets **110**, 3107 (2009). 10.1016/j.nds.2009.10.004
[37] M. Bender,et al., Phys. Rev. C **73**, 034322 (2006). 10.1103/PhysRevC.73.034322
[38] L. Robledo, et al., J. Phys. G: Nucl. Part. Phys. **46**, 013001 (2018). 10.1088/1361-6471/aadebd
[39] J.M. Pearson,et al., MNRAS **481**, 2994 (2018). 10.1093/mnras/sty2413
[40] O. Just, et al., Astrophys. J. Lett. **951**, L12 (2023). 10.3847/2041-8213/acdad2
[41] S. Goriely, Astron. Astrophys. **342**, 881 (1999)
[42] S. Goriely, et al., Phys. Rev. C **78**, 064307 (2008). 10.1103/PhysRevC.78.064307
[43] S. Goriely,et al., Phys. Rev. C, submitted (2024)
[44] S. Hilaire, et al., Phys. Lett. B **843**, 137989 (2023). 10.1016/j.physletb.2023.137989
[45] I. Dillmann, et al., AIP Conf. Proc. **819**, 123 (2006). 10.1063/1.2187846
[46] K. Sieja, Eur. Phys. J. A **59**, 147 (2023). 10.1140/epja/s10050-023-01067-8
[47] M. Frosini, et al., Phys. Rev. C **110**, 014307 (2024). 10.1103/PhysRevC.110.014307
[48] S. Goriely, et al.Eur. Phys. J. A **55**, 172 (2019). 10.1140/epja/i2019-12840-1
[49] M. Bender, et al., J. Phys. G: Nucl. Part. Phys. **47**, 113002 (2020). 10.1088/1361-6471/abab4f
[50] S. Goriely, et al., Phys. Rev. C **75**, 064312 (2007). 10.1103/PhysRevC.75.064312
[51] J.F. Lemaître, et al., Phys. Rev. C **98**, 024623 (2018). 10.1103/PhysRevC.98.024623
[52] A.J. Koning, J. Delaroche, Nuc. Phys. A **713**, 231 (2003). 10.1016/S0375-9474(02)01321-0
[53] J. Jeukenne, et al., Phys. Rev. C **16**, 80 (1977). 10.1103/PhysRevC.16.80
[54] E. Bauge, et al., Phys. Rev. C **63**, 024607 (2001). 10.1103/PhysRevC.63.024607
[55] L. McFadden, G. Satchler, Nucl. Phys. **84**, 177 (1966). 10.1016/0029-5582(66)90441-X
[56] D. Basak, C. Basu, Eur. Phys. J. A **58**, 150 (2022). 10.1140/epja/s10050-022-00798-4
[57] P. Demetriou, et al., Nucl. Phys. A **707**, 253 (2002). 10.1016/S0375-9474(02)00756-X
[58] V. Avrigeanu, et al., Phys. Rev. C **90**, 044612 (2014). 10.1103/PhysRevC.90.044612
[59] P. Mohr, et al., At. Data Nuc. Data Tables **142**, 101453 (2021). 10.1016/j.adt.2021.101453
[60] A. Choplin, et al., Astron. Astrophys. **661**, A86 (2022). 10.1051/0004-6361/202243331
[61] E. Somorjai, et al., Astron. Astrophys. **333**, 1112 (1998)